2016-05-31

Endothelial Mitogen-Activated Protein Kinase Kinase Kinase Kinase 4 Is Critical for Lymphatic Vascular Development and Function

Rachel J. Roth Flach
University of Massachusetts Medical School

Et al.

AMERICAN SOCIETY FOR MICROBIOLOGY | Molecular and Cellular Biology

Endothelial Mitogen-Activated Protein Kinase Kinase Kinase Kinase 4 Is Critical for Lymphatic Vascular Development and Function

Rachel J. Roth Flach,* Chang-An Guo,* Laura V. Danai,* Joseph C. Yawe, Sharvari Gujja, Yvonne J. K. Edwards, Michael P. Czech

Program in Molecular Medicine, University of Massachusetts Medical School, Worcester, Massachusetts, USA

The molecular mechanisms underlying lymphatic vascular development and function are not well understood. Recent studies have suggested a role for endothelial cell (EC) mitogen-activated protein kinase kinase kinase kinase 4 (Map4k4) in developmental angiogenesis and atherosclerosis. Here, we show that constitutive loss of EC Map4k4 in mice causes postnatal lethality due to chylothorax, suggesting that Map4k4 is required for normal lymphatic vascular function. Mice constitutively lacking EC Map4k4 displayed dilated lymphatic capillaries, insufficient lymphatic valves, and impaired lymphatic flow; furthermore, primary ECs derived from these animals displayed enhanced proliferation compared with controls. Yeast 2-hybrid analyses identified the Ras GTPase-activating protein Rasa1, a known regulator of lymphatic development and lymphatic endothelial cell fate, as a direct interacting partner for Map4k4. Map4k4 silencing in ECs enhanced basal Ras and extracellular signal-regulated kinase (Erk) activities, and primary ECs lacking Map4k4 displayed enhanced lymphatic EC marker expression. Taken together, these results reveal that EC Map4k4 is critical for lymphatic vascular development by regulating EC quiescence and lymphatic EC fate.

The vascular system is comprised of arteries and veins, which deliver nutrients to organs via capillaries and lymphatic vessels, which in turn reabsorb fluid from tissues for delivery back into the circulation. Both blood and lymphatic vessels are lined with endothelial cells (ECs), which are critical for the function and maintenance of both vascular networks (1). Normal lymphatic vascular function is required for maintaining fluid balance, immune surveillance, and lipid homeostasis (2, 3). In contrast, lymphatic vascular dysfunction is associated with numerous diseases, including developmental abnormalities, cancer metastasis, and lymphedema (4, 5). Though common pathways are involved in early vascular development, specialized molecules are required to drive and maintain lymphatic endothelial cell fate specification both during and after development (6, 7), and the signaling pathways that specifically promote lymphatic vascular development are still not well understood.

Our laboratory recently demonstrated that mitogen-activated protein kinase kinase kinase kinase 4 (Map4k4) has a profound role within the endothelium to promote atherosclerosis development and lymphocyte recruitment in inducible, endothelium-specific Map4k4 knockout animals on an *Apoe*$^{-/-}$ background (8). The present studies were designed to investigate the role of Map4k4 in endothelial cell function in more detail. We observed that mouse pups lacking endothelial Map4k4 displayed postnatal lethality due to chyle leakage into the thoracic cavity after birth (chylothorax) when constitutively expressed Cdh5 Cre (Ve-cadherin Cre) (9) was used to delete Map4k4 in the endothelium. Furthermore, animals constitutively lacking EC Map4k4 displayed dilated lymphatic capillaries, abnormal valves, and impaired lymphatic flow. Yeast 2-hybrid analysis of Map4k4 identified the protein RAS p21 protein activator 1 (Rasa1), which is critical for lymphatic development and is a negative regulator of Ras–mitogen-activated protein kinase (Ras-MAPK) signaling (10), as a direct binding partner for Map4k4. Loss of Map4k4 in ECs enhanced Ras and extracellular signal-regulated kinase (Erk) activities and ameliorated EC quiescence in culture. Taken together, these results demonstrate a complex and critical role for lymphatic endothelial Map4k4 in development.

MATERIALS AND METHODS

Mouse models. The University of Massachusetts Medical School Institutional Animal Care and Use Committee approved all of the animal procedures. Map4k4 Flox/Flox animals, Cdh5 Cre animals [B6.Cg-Tg(Cdh5-cre)7Mlia/J; Jackson Laboratories], and Map4k4 inducible endothelial cell-specific knockout (iECKO) mice [Cdh5(PAC)-CreERT2] have been previously described (8). At 6 to 8 weeks of age, male Flox/Flox and Flox/Flox/Cre^{+} littermates were injected with 1 mg tamoxifen/day in corn oil (Sigma) for 5 days and maintained on a chow diet. The mice were euthanized by CO_2 inhalation, followed by bilateral pneumothorax or by decapitation if younger than postnatal day 12 (p12). Footpads were injected with 25 μl of 2% Evans blue dye (Sigma) in phosphate-buffered saline (PBS), and lymph nodes were visualized 1 h later. No statistical methods were used to predict sample size, no randomization was performed, and the investigations were not blinded.

Cell culture and transfection. Human umbilical vein endothelial cells (HUVECs) and human dermal lymphatic endothelial cells (HDLECs) were purchased from Clonetics and grown in endothelial growth medium 2 (EGM-2) or EGM-2 microvascular (EGM-2MV) medium, respectively. The cells were transfected and maintained as previously described (8). Primary mouse lung endothelial cells (MLECs) were prepared by digestion and immune isolation, as previously described (8). The adenoviruses used for overexpression were a generous gift from Diane Barber (11).

Received 1 January 2016 **Returned for modification** 2 February 2016
Accepted 30 March 2016

Accepted manuscript posted online 4 April 2016

Citation Roth Flach RJ, Guo C-A, Danai LV, Yawe JC, Gujja S, Edwards YJK, Czech MP. 2016. Endothelial mitogen-activated protein kinase kinase kinase kinase 4 is critical for lymphatic vascular development and function. Mol Cell Biol 36:1740–1749. doi:10.1128/MCB.01121-15.

Address correspondence to Rachel J. Roth Flach, Rachel.Rothflach@pfizer.com, or Michael P. Czech, Michael.Czech@umassmed.edu.

* Present address: Rachel J. Roth Flach, Pfizer, Cambridge, Massachusetts, USA; Chang-An Guo, Department of Biochemistry, University of Wisconsin—Madison, Madison, Wisconsin, USA; Laura V. Danai, Koch Institute for Integrative Cancer Research, Massachusetts Institute of Technology, Cambridge, Massachusetts, USA.

HUVECs were infected with 0.25 μl virus/ml medium for 4 h and lysed 48 h after infection.

RNA isolation and quantitative RT-PCR. Total RNA was isolated, cDNA was prepared, and quantitative reverse transcription (qRT)-PCR was performed as previously described (8). The primer sequences were as follows: *Map4k4* F, CATCTCCAGGGAAATCCTCAGG, and R, TTCTGTA GTCGTAAGTGGCGTCTG; *Cd31* F, ACGCTGGTGCTCTATGCAAG, and R, TCAGTTGCTGCCCATTCATCA; *Cdh5* F, CACTGCTTTGGGAGCC TTC, and R, GGGGCAGCGATTCATTTTTCT; *Kdr* F, TTTGGCAAATA CAACCCTTCAGA, and R, GCAGAAGATACTGTCACCACC; *Lyve1* F, CAGCACACTAGCCTGGTGTTA, and R, CGCCCATGATTCTGCATG TAGA; *Prox1* F, AGAAGGGTTGACATTGGAGTGA, and R, TGCGTGT TGCACCACAGAATA; *Flt4* F, CTGGCAAATGGTTACTCCATGA, and R, ACAACCCGTGTGTCTTCACTG; *Sox18* F, CCTGTCACCAACGTCT CGC, and R, GCAACTCGTCGGCAGTTTG; *Pdpn* F, ACCGTGCCAGT GTTGTTCTG, and R, AGCACCTGTGGTTGTTATTTTGT; *Vegfc* F, GA GGTCAAGGCTTTTGAAGGC, and R, CTGTCCTGGTATTGAGGG TGG; and *Ccnd2* F, GAGTGGGAACTGGTAGTGTTG, and R, CGCACA GAGCGATGAAGGT.

Western blotting. Cells were lysed in lysis buffer (150 mM NaCl, 100 mM Tris, 5 mM EDTA, 1% Triton X-100 for cell lysates; 100 mM NaCl, 100 mM Tris, 5 mM EDTA, 1% Triton X-100 for immunoprecipitations) with 1× HALT protease and phosphatase inhibitors (Thermo Scientific). The lysates were run on SDS-PAGE gels and transferred to nitrocellulose membranes. The lysates were immunoprecipitated with anti-Ras GTPase-activating protein (GAP) antibodies (Santa Cruz; 2 μg) or anti-mouse IgG (2 μg). The membranes were immunoblotted with anti-MAP4K4 A301-503A (Bethyl; 1:2,000), phosphorylated-Erk (P-Erk) 4370 (Cell Signaling Technology; 1:1,000), total Erk1 sc-93 (Santa Cruz; 1:1,000), Rasa1/Ras GAP (Santa Cruz B4-F8; 1:250), or Ras (Thermo-Pierce; 1:200) antibodies.

Immunostaining. Whole-mount immunostaining was performed on tissues that had been fixed in 10% formalin for 2 to 6 h. Retinas were blocked overnight in 10% bovine serum albumin (BSA) and 0.3% Triton X-100 in PBS at 4°C; stained overnight with Isolectin B4 (Life Technologies; I21411; 1:40) in 100 mM $MgCl_2$, 100 mM $CaCl_2$, 10 mM $MnCl_2$, and 1% Triton X-100 in PBS at 4°C; and washed 3 times for 20 min each time in 5% BSA, 0.15% Triton X-100 in PBS at room temperature. von Willebrand factor (vWf) (Abcam ab9378; 1:200), Lyve-1 (Abcam 14917; 1:500), and Prox-1 (Abcam 37128; 1:200) immunostaining was performed in 3% goat serum and 2% BSA in 0.3% Triton overnight, followed by fluorescent secondary antibodies (Life Technologies). Tissues were mounted in ProLong Gold (Life Technologies). Whole-mount images were visualized in flattened 25-μm z-stacks with a Solamere Technology Group modified Yokogawa CSU10 spinning-disk confocal system with a Nikon TE-2000E2 inverted microscope at ×10 or ×20 magnification. Images were acquired with MetaMorph software, version 6.1 (Universal Imaging, Downingtown, PA). A Zeiss Axiovert 100 inverted microscope with a 5× or 10× objective and an AxioCam HRm camera was used for retina and intestine images. The images were quantified using ImageJ analysis software.

Proliferation assays. Primary MLECs were used at passage 3 for all experiments. For cell-counting assays, 25,000 cells were plated in 24-well plates on day 0. On day 1, the cells were trypsinized and counted. On days 2 to 4, the cells were trypsinized and counted, and this value was normalized to the count from day 1. Cell numbers were expressed as fold change from day 1. In parallel, equal numbers of MLECs were plated on 6-well plates. To assess proliferation, the cells were stained for Ki67 (phycoerythrin [PE]; BD) after a rest period. Apoptosis was induced by starving confluent MLECs for 72 h as described previously (10), and serum-fed or starved cells were stained with an annexin V apoptosis assay kit (BD) according to the manufacturer's instructions. Cell cycle analysis was performed using a fluorescein isothiocyanate (FITC) bromodeoxyuridine (BrdU) flow kit (BD) according to the manufacturer's instructions. The data were collected on an LSRII flow cytometer (BD) and were analyzed with FlowJo software. Samples were gated for scatter and single cells. Gates were drawn based on fluorescence minus one (FMO) controls. A total of at least 100,000 events were recorded.

Ras-GTP levels. HUVECs were transfected with scrambled or MAP4K4 small interfering RNA (siRNA), as previously reported (8). The cells were serum starved overnight prior to the assay. The active Ras pull-down and detection kit (Thermo-Pierce) was used according to the assay instructions. Briefly, glutathione *S*-transferase (GST)–Raf1 was used to pull down active Ras from cell lysates with glutathione beads, and the amount of active Ras in the pulldowns was normalized to that in cell lysates.

Yeast 2-hybrid assay. The Clontech Matchmaker gold yeast 2-hybrid system was used to screen a whole mouse genome library. A 31.5-kDa fragment of murine Map4k4 encoding the N-terminal kinase domain or a 39.5-kDa fragment of murine Map4k4 encoding the C-terminal citron homology domain (CNH) was cloned into the pGBKT7 plasmid using the In-Fusion advantage kit (Clontech) and used as bait. Screening and binding partner identification was performed according to the assay instructions.

Fluid biochemical analysis. Fluid was collected from the thoracic cavity, and blood was collected via cardiac puncture from the same Map4k4 Cdh5 Cre animals prior to death. Triglyceride (Sigma) and cholesterol (Pointe Scientific) contents were assessed by colorimetric methods, and albumin (Abcam) and fibrinogen (Abcam) contents were assessed by enzyme-linked immunosorbent assay (ELISA). Values were obtained for both fluids, and a ratio (thoracic fluid/blood) was calculated from the values obtained. Colorimetric assays and ELISAs were performed according to the manufacturers' instructions.

Microarray analysis. RNA was isolated, using TriPure (Roche), from three independent experiments, and cDNA synthesis and *in vitro* transcription were performed using the Ambion WT expression kit (Ambion, Carlsbad, CA). Second-strand cDNA was labeled with the Affymetrix WT terminal-labeling kit, and samples were hybridized to three different Affymetrix Genechip Human Gene 1.0 ST arrays. The Microarray Computational Environment (MACE) was used to process raw oligonucleotide microarray data as previously described (12), and KEGG analysis was performed in MACE internally using the R package KEGG.db.

Statistical analysis. For the microarray, the differential expression analysis of genes in two groups was performed using Student's *t* test internally within MACE (12). A two-tailed Student *t* test was used to compare two groups in Microsoft Excel. Two-way analysis of variance (ANOVA) with the Sidak posttest was used to compare multiple groups in GraphPad Prism 6.0. A P value of <0.05 was considered to be statistically significant. Variance was estimated using the standard error of the mean.

Microarray data accession number. The data described in this article are accessible via GEO series accession no. GSE78107 (http://www.ncbi.nlm.nih.gov/geo/query/acc.cgi?acc=GSE78107).

RESULTS

Mice lacking endothelial Map4k4 display lymphatic defects. Previous studies conducted in our laboratory to assess the role of Map4k4 in the endothelium utilized mice with endothelium-specific short hairpin RNA (shRNA)-mediated constitutive Map4k4 knockdown or inducible endothelial cell-specific Map4k4 Flox/Flox animals (8). We observed during the course of these studies that mice constitutively lacking endothelial Map4k4, which were developed by crossing Map4k4 Flox/Flox animals to Ve-cadherin Cre animals (Map4k4 Cdh5 Cre), did not survive past weaning age. Though these mice were born at nearly Mendelian ratios (Table 1), less than 5% of Map4k4 Cdh5 Cre mice survived to weaning age, and the median time of death was p9 (Fig. 1A).

Map4k4 Cdh5 Cre animals displayed rapid, shallow breathing prior to death, and upon dissection, a milky white fluid was observed in the thoracic cavities of these animals (Fig. 1B). Though

TABLE 1 Predicted genotypes of pups[a]

Genotype	Predicted		Actual	
	No.	%	No.	%
flox/+	37.5	25	54	36
flox/flox	37.5	25	34	22.7
flox/+ cdh5 cre	37.5	25	33	22
flox/flox cdh5 cre	37.5	25	23	15.3

[a] Map4k4 *flox/flox cdh5 cre* pups born compared with the predicted Mendelian ratio ($n = 150$).

this fluid was often acellular (Fig. 1C), we performed biochemical analyses to compare the properties of the thoracic fluid to those of the blood. We observed that the triglyceride content in the thoracic fluid was much higher, concomitant with lower levels of cholesterol and fibrinogen than in blood from the same animals (Table 2). The properties of the thoracic fluid were consistent with that of chylous leakage, which led us to conclude that the animals succumbed to chylothorax.

The chyle leakage observed in Map4k4 Cdh5 Cre animals suggested that the lymphatic vascular system might be affected in these animals. The lymphatic vascular system is comprised of a network of lymphatic capillaries, which drain fluid containing plasma proteins and immune cells in response to changes in interstitial pressure, and lacteals in the small intestine that absorb dietary lipids as chylomicrons (2, 4, 5). Thus, to assess the lymphatic vascular morphology, immunostaining for Lyve-1, a lymphatic capillary marker, was performed in the ear skin and mesenteries of Flox/Flox and Map4k4 Cdh5 Cre animals. While a typical network of lymphatic capillaries was observed in Flox/Flox mice, Map4k4 Cdh5 Cre animals displayed a 57% increase in lymphatic vascular density, which was attributed in part to a 58% increase in the lymphatic vascular diameter (Fig. 2A to C). Similarly, a 60% increase in the Lyve-1-positive area and a 51% increase in the Lyve-1-positive-vessel diameter was observed in Map4k4 Cdh5 Cre intestinal cross sections compared with controls (Fig. 3D to F).

Lymphatic capillaries drain into larger collecting vessels, which pump chyle against gravity into the thoracic duct and eventually into the venous circulation (4, 13). Chyle backflow from these collecting vessels is prevented by a series of valves (14). To assess the valve morphology, immunostaining with Prox-1, a lymphatic marker that concentrates at lymphatic valves (15), was performed in the mesenteries of p2 Flox/Flox and Map4k4 Cdh5 Cre animals. Prox-1 staining in Flox/Flox animals revealed a typical V-like shape, indicating lymphatic valves. However, in Map4k4 Cdh5 Cre mice, Prox-1 immunostaining revealed abnormal Prox-1 localization, and the majority of lymphatic valves displayed an altered, open morphology (Fig. 2D). Furthermore, there was a 61% reduction in the number of valves per millimeter mesentery in Map4k4 Cdh5 Cre animals (Fig. 2E). These results indicate that endothelial Map4k4 is critical for lymphatic-valve development, and thus, Map4k4 depletion manifests in dilated lymphatic capillaries and lymphatic leakage.

To assess lymphatic function, Evans blue dye was injected into one rear footpad of live p16 Flox/Flox and Map4k4 Cdh5 Cre mice. In Flox/Flox animals, the dye migrated to the inguinal and iliac lymph nodes in a typical pattern within 60 min postinjection. However, in Map4k4 Cdh5 Cre mice, the dye did not migrate to the iliac lymph node, and while dye was observed in the inguinal lymph node, an excess of dye was observed throughout the skin capillaries (Fig. 2F to G). These data demonstrate that Map4k4 Cdh5 Cre lymphatic vessels do not pump fluid sufficiently, thus promoting fluid stasis and accumulation within superficial lymphatic capillaries.

Previous reports suggested a role for endothelial Map4k4 in developmental angiogenesis using endothelium-specific Tie2 Cre, Rosa26-inducible whole-body deletion, and pharmacological inhibitors (16). To assess developmental vascularization in Map4k4 Cdh5 Cre mice, isolectin B4 (iB4) staining of p6 Flox/Flox and Map4k4 Cdh5 Cre retinas was performed. Similar to the previous study, we also observed reduced retinal outgrowth (enhanced avascular area), as well as increased vascular density in Map4k4 Cdh5 Cre mice compared with controls (Fig. 3A to C). However, no alterations in intestinal blood vessel area or diameter were observed, as assessed by vWf immunostaining (Fig. 3G to I). These data suggest that loss of Map4k4 using Cdh5 Cre results in only mild blood vascular phenotypes.

Enhanced EC proliferation in Map4k4 iECKO mice. The enhanced lymphatic and blood vascular density phenotypes observed in development (Fig. 2 and 3) suggested that Map4k4 may affect EC growth. Thus, primary MLECs were isolated from adult C57BL/6J Map4k4 Flox/Flox or Map4k4 inducible EC-specific knockout iECKO) mice, which have been previously described (8). To functionally assess whether ECs lacking Map4k4 displayed an enhanced capacity to proliferate, subconfluent Flox/Flox and Map4k4 iECKO primary MLECs were plated and counted daily for 4 days in parallel. Whereas the doubling time of Flox/Flox MLECs was 60.1 h, Map4k4 iECKO MLECs doubled 33% faster (45.0 h), which was significantly increased from controls (Fig. 4A). Furthermore, this enhancement in proliferation was accompanied by nearly a 2-fold increase in expression of the proliferation marker Ki67 in Map4k4 iECKO MLECs compared with Flox/Flox MLECs (Fig. 4B). The changes observed in

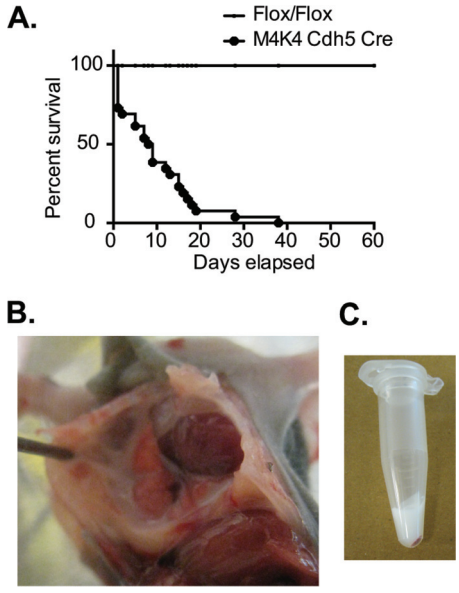

FIG 1 Mice constitutively lacking EC Map4k4 develop chylothorax. (A) Map4k4 (M4K4) Cdh5 Cre animals die at a median of p8.5 ($n = 26$; $P < 0.0001$). (B) Map4k4 Cdh5 Cre animal at p7 displaying chylothorax. (C) Fluid from the thoracic cavity of a representative Map4k4 Cdh5 Cre animal.

TABLE 2 Biochemistry of thoracic fluid[a]

	Triglycerides			Cholesterol			Albumin			Fibrinogen		
	Amt (mg/dl)			Amt (mmol/liter)			Amt (g/liter)			Amt (mg/liter)		
Mouse	Thoracic fluid	Blood	Ratio	Thoracic fluid	Blood	Ratio	Thoracic fluid	Blood	Ratio	Thoracic fluid	Blood	Ratio
1	149.2	66.6	2.2	64.0	100.8	0.6	26.3	33.6	0.8	867.4	1,115.1	0.8
2	230.6	162.7	1.4	54.5	103.2	0.5	26.4	34.8	0.8	858.4	939.6	0.9
3	276.8	98.0	2.8	56.2	101.1	0.6	25.5	35.6	0.7	875.7	1,096.4	0.8
4	566.6	133.3	4.3	124.5	203.1	0.6	25.1	24.0	1.0	816.7	949.6	0.9
5	1,354.5	100.7	13.4	95.6	105.8	0.9	26.7	23.4	1.1	884.6	1,036.9	0.9
6	537.6	239.7	2.2	122.8	219.6	0.6	25.9	25.2	1.0	862.4	1,199.1	0.7

[a] Peripheral blood and fluid from the thoracic cavity were collected from Map4k4 Cdh5 Cre pups prior to death. The ratios of the amounts of analytes in the thoracic fluid to those in the blood are shown.

cell numbers were not due to apoptosis, as annexin V staining was not altered between genotypes (Fig. 4C). These results suggest that Map4k4 depletion in ECs results in increased hyperplasia due to enhanced proliferation.

To elucidate how Map4k4 altered proliferation, the cell cycle of primary MLECs derived from Flox/Flox and Map4k4 iECKO mice was assessed using BrdU and 7-aminoactinomycin D (7-AAD) incorporation. After an overnight pulse of BrdU, similar percent-

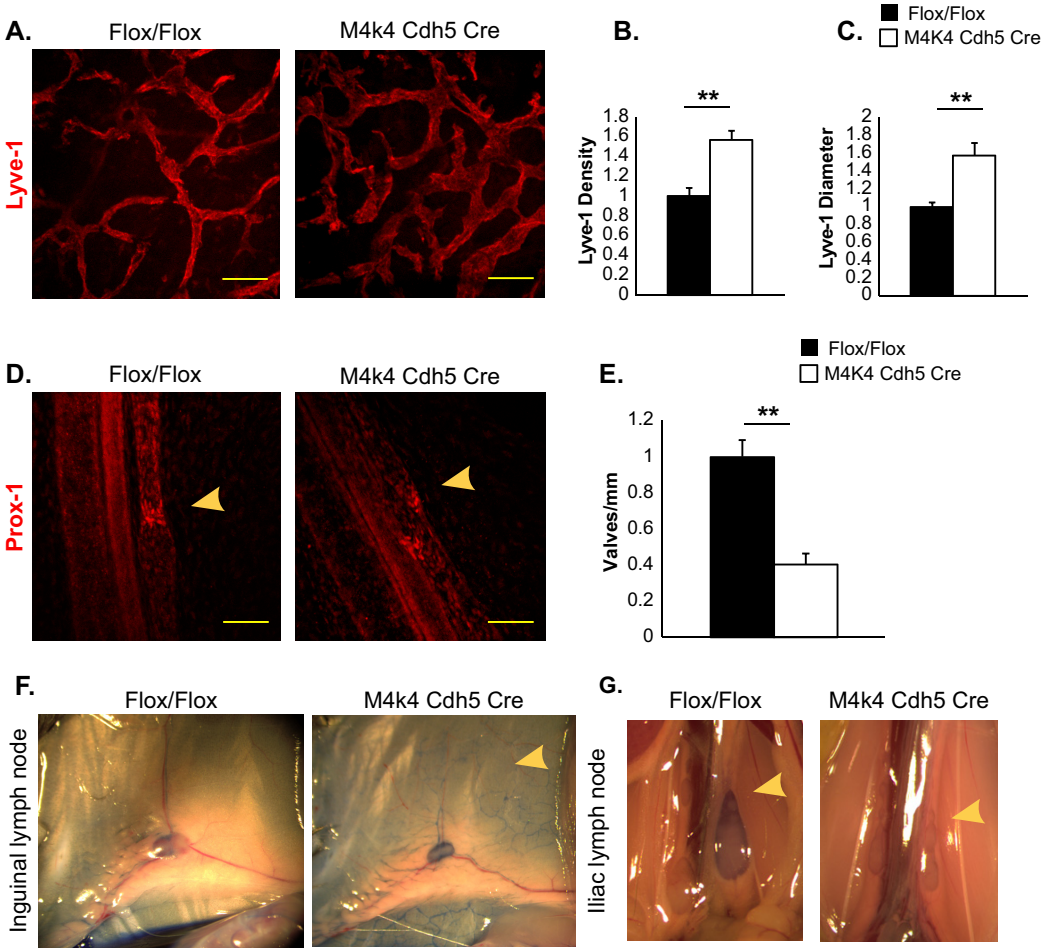

FIG 2 Lymphatic abnormalities in Map4k4 Cdh5 Cre mice. (A to C) Ear skin from p6 Flox/Flox or Map4k4 Cdh5 Cre animals was stained with Lyve-1 as a marker of lymphatic capillaries. (A) Representative images. Scale bars, 100 μm. (B) Vessel density as a measure of percent stained area normalized to the Flox/Flox area. (C) Average vessel diameter as normalized to the Flox/Flox diameter. (D and E) Mesenteries from p2 Flox/Flox or Map4k4 Cdh5 Cre animals were stained with Prox-1 as a marker of lymphatic valves. (D) Representative images. The arrowheads indicate valves. Scale bars, 100 μm. (E) Numbers of valves per millimeter mesentery as normalized to Flox/Flox animals. (F and G) p16 pups were injected with Evans blue dye in the footpad, and the mice were sacrificed to visualize dye in lymph nodes 1 h later. The images are representative of at least 4 animals per genotype. (F) Inguinal lymph nodes; the arrowhead indicates enhanced capillary visualization in the skin of Map4k4 Cdh5 Cre mice. (G) Iliac lymph nodes; the arrowheads indicate a lack of dye in iliac lymph nodes of Map4k4 Cdh5 Cre mice. The error bars represent standard errors of the mean. **, $P < 0.005$; $n = 4$ to 6.

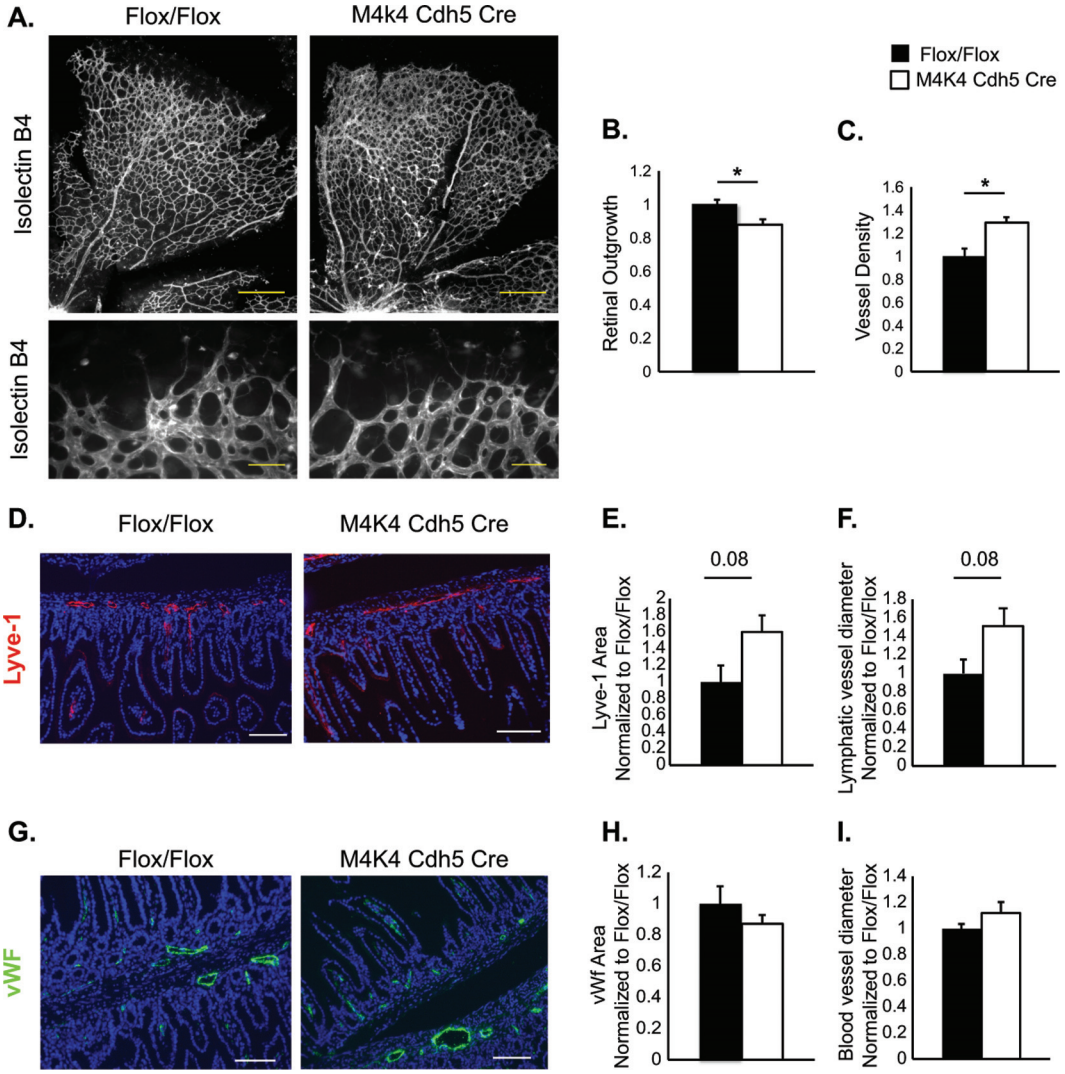

FIG 3 Vascular abnormalities in Map4k4 Cdh5 Cre mice. (A to C) Retinas were isolated from p6 Flox/Flox or Map4k4 Cdh5 Cre pups and stained with isolectin B4. (A) Representative images (×5 magnification, scale bars = 250 μm [top]; ×20 magnification, scale bars = 50 μm [bottom]). (B) Quantitation of retinal outgrowth as the diameter from the optic nerve to the perimeter as normalized to Flox/Flox (*, $P < 0.05$; $n = 5$ or 6). (C) Vessel density quantified as percent stained area and normalized to Flox/Flox (*, $P < 0.05$; $n = 6$ or 7). (D to I) Intestines were isolated from p18 Flox/Flox or Map4k4 Cdh5 Cre pups. (D to F) Intestinal cross sections were stained with Lyve-1 as a lymphatic capillary marker and with 4′,6-diamidino-2-phenylindole (DAPI) to visualize villi. (D) Representative images; scale bars, 50 μm. (E) Quantitation of Lyve-1-stained area as normalized to Flox/Flox animals. (F) Quantitation of Lyve-1-stained-vessel diameter as normalized to Flox/Flox animals ($n = 4$ to 6). (G to I) Intestinal cross sections were stained with vWF as a blood endothelial marker and with DAPI to visualize villi; scale bars, 50 μm. (G) Representative images. (H) Quantitation of vWF-stained area as normalized to Flox/Flox animals. (I) Quantitation of vWF-stained-vessel diameter as normalized to Flox/Flox animals ($n = 4$ to 6). The error bars represent standard errors of the mean.

ages of MLECs were identified in G_0/G_1 and S phases of the cell cycle; however, there was a significant (30%) reduction of Map4k4 iECKO MLECs in the G_2/M transition ($BrdU^-$ $7\text{-}AAD^+$; 28% Flox/Flox versus 16% Map4k4 iECKO) (Fig. 4D). These data suggest that loss of Map4k4 in ECs alters cell cycle progression.

To identify whether loss of Map4k4 in ECs altered cell cycle gene expression, a microarray analysis was performed in HUVECs after treatment with scrambled or MAP4K4 siRNA. Of the genes regulated by MAP4K4 loss, several were involved in cell cycle regulation, G_2/M transition, and mitosis (Fig. 4E). KEGG analysis of the most highly up- or downregulated (>|1.5|-fold) genes revealed that loss of MAP4K4 affected the following pathways: cell cycle ($P = 2 \times 10^{-6}$), p53 signaling ($P = 5 \times 10^{-4}$), oocyte meiosis ($P = 0.001$), progesterone-mediated oocyte maturation ($P = 0.001$), hematopoietic cell lineage ($P = 0.002$), and cytokine-cytokine receptor interaction ($P = 0.05$).

Cell cycle gene expression was also affected by Map4k4 loss in MLECs, as Map4k4 iECKO MLECs demonstrated a significant 2-fold increase in *Ccnd2* mRNA expression compared with Flox/Flox controls (Fig. 4F). These data demonstrate that loss of Map4k4 in HUVECs and MLECs alters the expression of genes involved in cell cycle progression.

MAP4K4 directly binds RASA1 and negatively regulates ERK activity and lymphatic cell fate. To elucidate the molecular mechanisms by which Map4k4 operates in ECs, a yeast 2-hybrid screen was performed in which the NH_2-terminal kinase domain or the

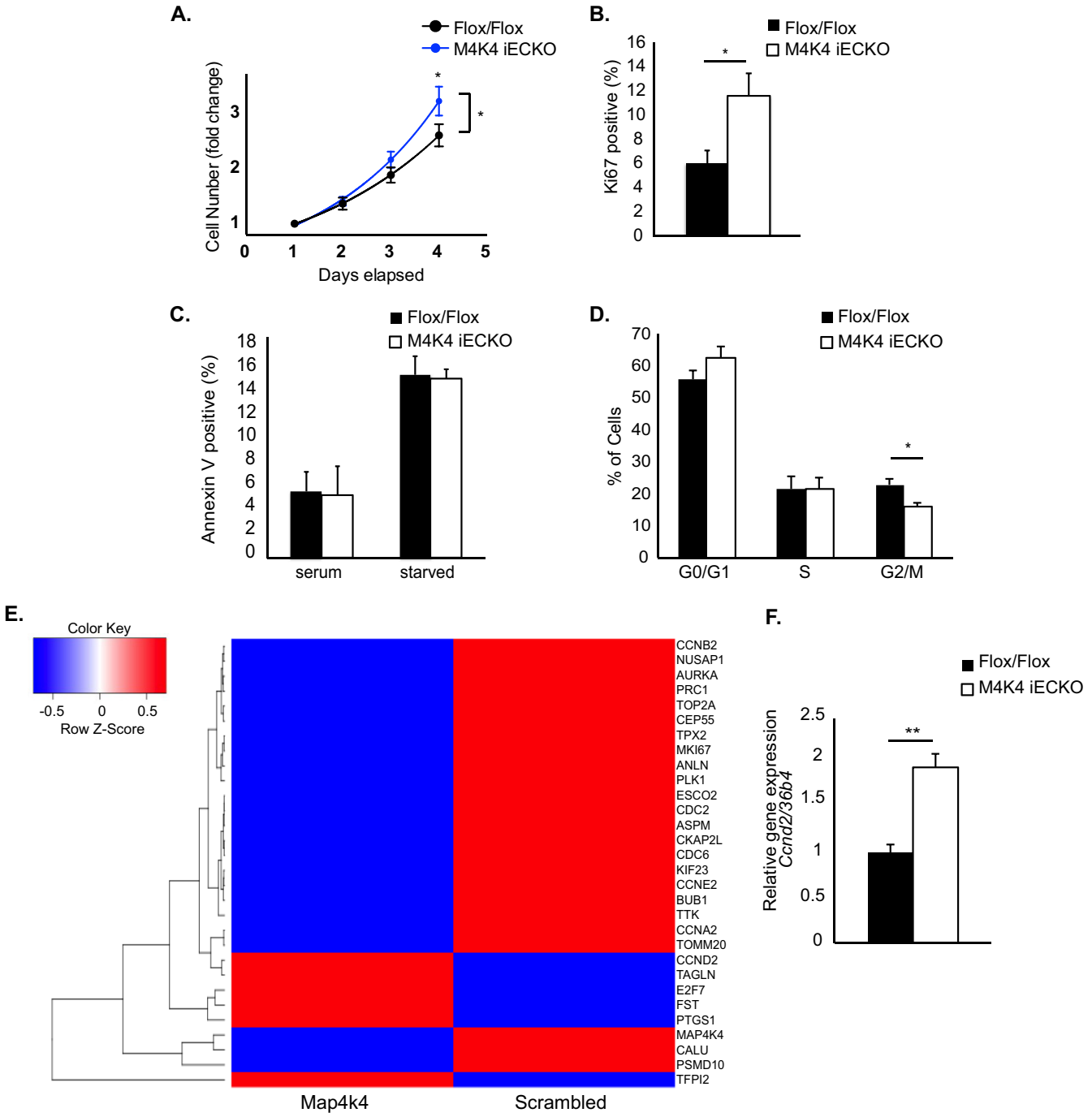

FIG 4 Enhanced proliferation in ECs lacking Map4k4. (A to D and F) Primary MLECs were derived from chow-fed Flox/Flox or Map4k4 iECKO mice. (A) MLECs were plated at subconfluence and counted daily. The cell counts were normalized to that of day 1 and expressed as fold change. (ANOVA; *, $P < 0.05$; $n = 7$ to 11). (B) Ki67 staining in MLECs as assessed by flow cytometry (*, $P < 0.05$; $n = 6$ or 7). (C) Annexin V staining in serum-fed or serum-starved MLECs as assessed by flow cytometry ($n = 6$ or 7). (D) The cell cycle was assessed by BrdU and 7-AAD staining using flow cytometry (G_0/G_1, $BrdU^-$ $7\text{-}AAD^-$; S, $BrdU^+$; G_2/M, $7\text{-}AAD^+$; *, $P < 0.05$; $n = 6$). (E) HUVECs were transfected with scrambled or Map4k4 siRNA, the cells were serum starved overnight, and a microarray analysis was performed. The heat map represents 30 of the most up- or downregulated genes after Map4k4 knockdown (|fold change| > 1.5). (F) *Ccnd2* expression was assessed in MLECs by qRT-PCR and normalized to that of *36b4* (**, $P < 0.005$; $n = 6$). The error bars represent standard errors of the mean.

C-terminal CNH domain of Map4k4 was used as bait to screen a whole-genome library. Though several unique hits were obtained using the kinase or the CNH domain (Table 3), we focused on Rasa1, a GAP for Ras (also known as p120 RasGAP), as an interacting partner of the CNH domain of Map4k4. We focused on Rasa1 for several reasons. First, previous studies have demonstrated direct and indirect interactions of Map4k4 and the adapter protein Nck (17), which directly binds Rasa1 (18). Second, an additional study demonstrated that Map4k4 is in a complex with Rasa1, although it was hypothesized in that study that the binding

TABLE 3 Yeast 2-hybrid screen results

Domain[a]	Occurrence[b]	Protein	Confirmed in yeast[c]
Kinase	44	von Hippel-Lindau binding protein (Vbp1)	Yes
Kinase	3	Filamin, alpha	Yes
Kinase	2	Fatty acid binding protein 4, adipocyte (Fabp4)	Yes
Kinase	1	Proliferation-associated 2G4 (Pa2g4)/Erb binding protein 1 (EBP1)	Yes
Kinase	3	CD48 antigen	No
Kinase	1	Ubiquitin-conjugating enzyme E2N	No
Kinase	1	HFM1; ATP-dependent DNA helicase homolog	ND
Kinase	1	Dynactin 4	No
Kinase	1	Glycine amidinotransferase (L-arginine::glycine amidinotransferase) (Gatm)	ND
Kinase	1	Complement component 4 binding protein (C4bp)	No
Kinase	2	Inter-alpha (globulin) inhibitor H5 (Itih5)	No
Kinase	2	Centrosome- and spindle pole-associated protein 1 (Cspp1)	ND
Kinase	1	Leukotriene A4 hydrolase (Lta4h)	No
Kinase	1	Nedd8 (neural precursor cell overexpressed developmentally downregulated gene 8)	ND
Kinase	1	Ribosomal protein S20 (Rps20)	ND
Kinase	2	Ras p21 protein activator 2 (Rasa2)	ND
Kinase	1	Riken cDNA 4932415G16 gene	ND
Kinase	1	*Mus musculus* titin (Ttn), transcript variant N2-A, transcript variant N2-B, mRNA	No
CNH	15	Proteasome (prosome and macropain) 26S subunit, ATPase, 6 (Psmc6)	Yes
CNH	10	Kruppel-like factor 4 (gut) (Klf4)	Yes
CNH	2	RAS p21 protein activator 1 (Rasa1)	ND
CNH	2	Cell division cycle 123 homolog (*Saccharomyces cerevisiae*) (Cdc123)	ND
CNH	2	Bromodomain PHD finger transcription factor (Bptf)/FALZ	ND
CNH	1	Bobby sox homolog (*Drosophila*) (Bbx)/HBP2	ND
CNH	1	Transcription factor 4 (Tcf4)	Yes
CNH	1	SUB1 homolog (*S. cervesiae*)	Yes
CNH	1	Annexin A8 (Anxa8)	Yes
CNH	1	Cspp1	ND

[a] The Clontech matchmaker gold yeast 2-hybrid system was used to screen a whole human genome library with the MAP4K4 N-terminal kinase domain (Kinase) or C-terminal CNH as bait.
[b] Occurrence, number of times a protein was identified in the screen.
[c] Confirmed in yeast indicates whether isolated clones were retransfected into yeast to verify the interaction. ND, not done.

of the two proteins was indirect (19). Third, RASA1 mutations are associated with lymphatic dysfunction in humans (20). Finally, inducible loss of Rasa1 in mice causes lymphatic vascular proliferation phenotypes, as well as chyle leakage and death, which is a phenotype similar to the one we observed in Map4k4 Cdh5 Cre mice (10, 20). Interestingly, mapping of the Y2H clone that interacted with Map4k4 determined that Map4k4 bound the GAP domain of Rasa1 (Fig. 5A), suggesting that Map4k4 may affect Rasa1 function to dampen Ras activity. We confirmed the association of RASA1 and MAP4K4 in HUVECs by immunoprecipitating endogenous RASA1 and immunoblotting overexpressed wild-type (WT) MAP4K4 or a MAP4K4 mutant that renders it kinase inactive (DN), which we expressed in an effort to form a more stable complex with RASA1 (Fig. 5B). Endogenous complex formation of RASA1 and MAP4K4 was also detected in HDLECs by coimmunoprecipitation (Fig. 5C).

Rasa1 promotes the hydrolysis of Ras-GTP to Ras-GDP and thus inactivates the Ras-Erk cascade (21). To determine whether MAP4K4 affected Ras-MAPK pathway levels or activity, HUVECs were transfected with scrambled or MAP4K4 siRNA for 48 h. Notably, there were no alterations in total levels of RASA1 after MAP4K4 depletion (Fig. 5D). The cells were serum starved, and RAS-GTP loading was assessed using GST-Raf1 to pull down active RAS. A 2-fold increase was observed in the amount of RAS bound to GST-Raf1 when normalized to total RAS levels after MAP4K4 silencing, suggesting that loss of MAP4K4 in ECs promotes basal RAS activation (Fig. 5E).

MAP4K4 silencing also led to increased p-ERK levels as normalized to total ERK in HUVECs (Fig. 5F), HDLECs (Fig. 5G), and MLECs (Fig. 5H) after serum starvation. However, acute VEGF-C stimulation induced transient ERK activation with similar temporal regulation in scrambled and MAP4K4 siRNA-transfected HUVECs and HDLECs, as well as primary MLECs lacking Map4k4 (Fig. 5F to H). These results suggest that MAP4K4 is critical to maintain EC quiescence at the level of ERK activation but is dispensable for growth factor-induced ERK activation.

The Ras-Erk axis controls lymphangiogenesis and cell fate by activating a series of genes that are necessary and sufficient to maintain a lymphatic EC signature, including the transcription factors Sox18 and Prox1 (22). Thus, we assessed whether loss of Map4k4 promoted a lymphatic endothelial cell fate, which may contribute to the chyle leakage phenotype that was observed (Fig. 1). Primary MLECs were isolated from Flox/Flox and Map4k4 iECKO mice, and qRT-PCR was performed for a number of endothelial marker genes. While expression of the pan-endothelial marker genes *Cd31*, *Cdh5*, and *Kdr* (Vegfr2) did not differ between genotypes, the lymphatic endothelial marker genes *Lyve1*, *Prox-1*, *Flt4* (Vegfr3), and *Sox18* were all upregulated in Map4k4 iECKO MLECs compared with Flox/Flox ECs, whereas no difference was observed in the collecting vessel marker gene *Pdpn* (Fig. 5I). Interestingly, reduced mRNA levels of *Vegf-c*, encoding a Vegfr3 ligand that promotes lymphatic endothelial fate and function, were observed in Map4k4 iECKO MLECs, suggesting that the cell

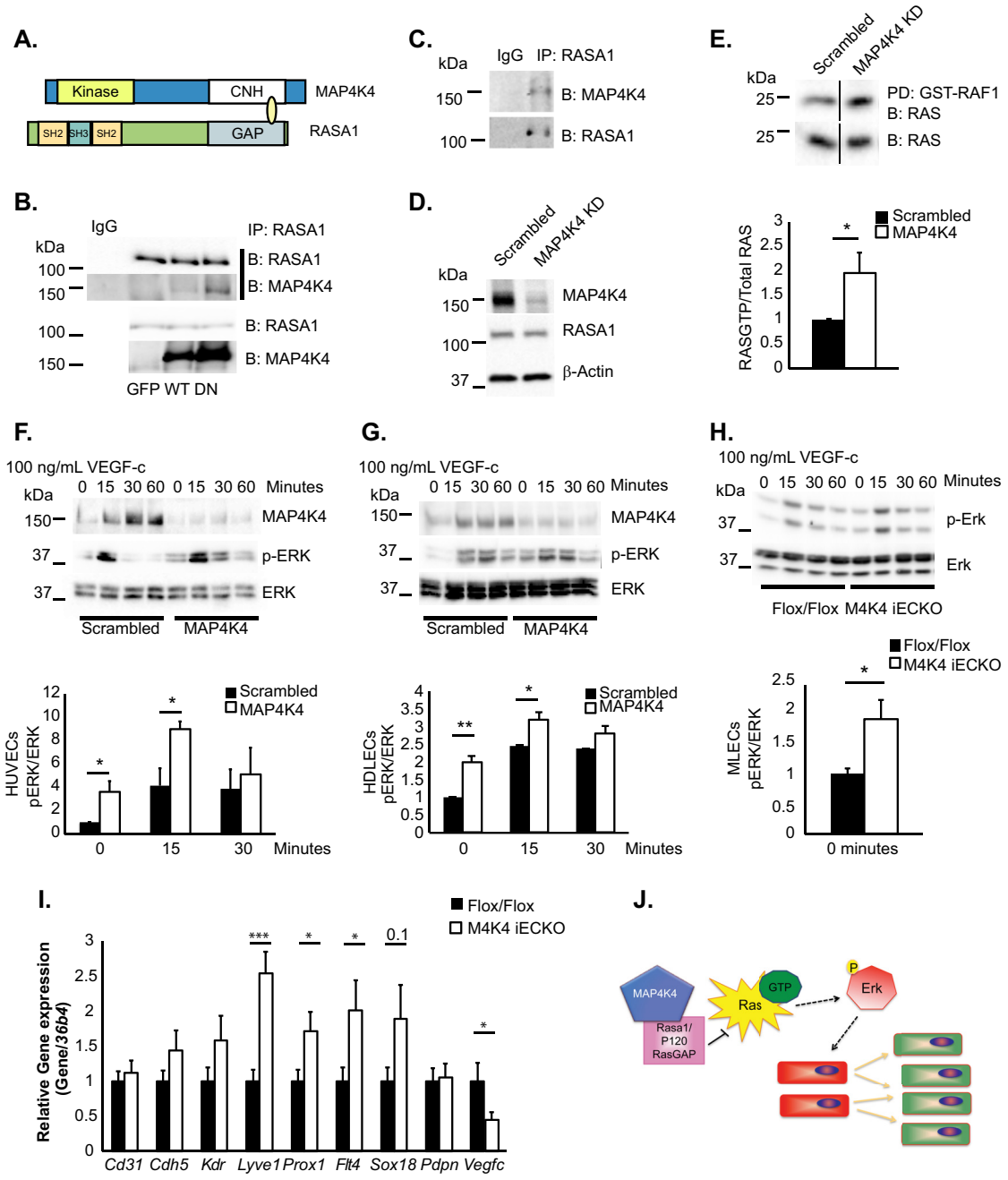

FIG 5 MAP4K4 binds to RASA1 and regulates basal RAS-ERK signaling. (A) Diagram of MAP4K4 and RASA1 domains that directly bound in a yeast 2-hybrid screen. (B) Coimmunoprecipitation of endogenous RASA1 and overexpressed MAP4K4 in HUVECs. The immunoblots are representative of the results of at least 3 independent experiments. (C) Immunoprecipitation of endogenous RASA1 and endogenous MAP4K4 in HDLECs. The immunoblots are representative of the results of at least 3 independent experiments. (D to G) ECs were treated with scrambled or MAP4K4 siRNA for 48 h. (D) RASA1 protein levels were assessed in HUVECs and normalized to β-actin (representative results; $n = 4$). (E) Ras-GTP levels were measured in serum-starved HUVECs by assessing GST-RAF1-bound RAS in pulldowns (top) as normalized to total RAS levels in cell lysates (bottom) by densitometry (*, $P < 0.05$; $n = 4$). The immunoblots were run on the same gel but in noncontiguous lanes. (F to H) HUVECs (F), HDLECs (G), and MLECs (H) were serum starved overnight and stimulated with 100 ng/ml VEGF-C in a time course. The lysates were immunoblotted for MAP4K4, p-ERK, and total ERK, and p-ERK levels were normalized to total ERK by densitometry (*, $P < 0.05$; **, $P < 0.005$; $n = 3$ or 4 HUVECs or HDLECs; $n = 7$ or 8 MLECs). (I) MLECs were isolated from chow-fed Flox/Flox or Map4k4 iECKO mice at least 16 weeks after tamoxifen injections, and the indicated genes were assessed by qRT-PCR and normalized to *36b4* (*, $P < 0.05$; ***, $P < 0.0005$; $n = 8$ to 13). (J) Model of the hypothesis. Map4k4 directly binds Rasa1 to negatively regulate Ras-GTP and Erk activity; thus, Map4k4 loss drives EC proliferation and a lymphatic endothelial cell fate switch, which promotes lymphatic dysfunction. The error bars represent standard errors of the mean.

fate effect may be unrelated to enhanced ligand production (Fig. 5I). Thus, Map4k4 is important for maintenance of EC fate and quiescence by modulation of the Ras-Erk signaling pathway. These results collectively are consistent with the observations that loss of endothelial Map4k4 *in vivo* causes lymphatic vascular hyperproliferation and leakage, resulting in developmental and functional abnormalities (Fig. 5G).

DISCUSSION

The major findings of the present study demonstrate that the endothelial protein kinase Map4k4 is required for lymphatic vascular development. Constitutive endothelial Map4k4 deletion using Cdh5/Ve-cadherin Cre revealed that Map4k4 has a fundamental role in lymphatic vascular development, as Map4k4 Cdh5 Cre mice displayed postnatal lethality (Fig. 1) due to chylothorax (Table 2), which was accompanied by lymphatic capillary dilation, reduced lymphatic collecting valve numbers, and impaired lymphatic flow (Fig. 2).

Recent studies by Vitorino et al. (16) used Tie2 Cre and Rosa26 deletion models to demonstrate that Map4k4 is important for developmental angiogenesis and retinopathy in mice. Though we observed delayed retinal outgrowth and enhanced vascular density in Map4k4 Cdh5 Cre retinas at p6, which was similar to the findings of Vitorino et al., no alteration in blood endothelial morphology or area was observed in the intestines of Map4k4 Cdh5 Cre mice (Fig. 3). Furthermore, these authors demonstrated lethality at embryonic day 16.5 (e16.5) in this model (16). Because the Tie2 Cre model deletes genes in endothelial cells earlier than Cdh5 (Ve-cadherin) (23), it is not surprising that Map4k4 Cdh5 Cre animals displayed delayed lethality (Fig. 1). Notably, although Vitorino et al. did not report any lymphatic phenotypes, edema was observed in Map4k4 Tie2 Cre knockout mice (16), which is indicative of lymphatic dysfunction (24).

Our previous studies using *Apoe*$^{-/-}$ mice determined that endothelial Map4k4 was critical for atherosclerosis development (8). Recent studies have demonstrated that the high plasma cholesterol content in *Apoe*$^{-/-}$ mice contributes to impaired lymphatic drainage, which is accompanied by lymphatic dysfunction and regression (25). However, follow-up studies reported an active role for the lymphatic vascular system in reverse cholesterol transport of lipid-laden macrophages in atherosclerosis; thus, the dysfunctional lymphatic network in hypercholesterolemic mice contributes to disease (26, 27). Though we did not observe chyle leakage phenotypes in mice lacking endothelial Map4k4 on an *Apoe*$^{-/-}$ background, we cannot rule out, based on the studies presented here, the possibility that the lymphatic endothelium is partially responsible for ameliorating atherosclerosis in *Apoe*$^{-/-}$ mice lacking endothelial Map4k4. Thus, future studies will investigate the role of reverse cholesterol transport in the improved atherosclerosis phenotypes observed in these animals, as well as a lymphatic-specific role for Map4k4 in atherosclerosis.

Among many proteins identified as Map4k4 binding partners in a yeast 2-hybrid screen (Table 3), Rasa1 was chosen for further assessment. Few mouse models display lymphatic dysfunction and chyle leakage, and these mice genetically map out a signaling pathway that is critical for lymphatic development and function, including gain or loss of Vegf-c or Vegfr3 (28, 29), loss or mutation of Ephrinb2 (30) or Ephb4 (31) and Rasa1 (10, 32), or gain of function of Ras and Erk (22, 33, 34). Furthermore, the similarity of the phenotypes of these animal models and mice lacking endothelial Map4k4 strongly suggested that Map4k4 functions within this signaling pathway. Indeed, Map4k4 was previously identified as an effector in the ephrin pathway *in vitro*, which forms a complex with Rasa1 (19). Consistent with the known actions of Rasa1 to inactivate Ras and Erk, enhanced Ras and Erk activities were observed basally when Map4k4 was knocked down in vascular and lymphatic ECs (Fig. 5). Furthermore, primary MLECs lacking Map4k4 proliferated more (Fig. 4), concomitant with a reduced population of cells in G_2/M transition and alterations in cell cycle gene expression (Fig. 4). Interestingly, a number of the genes affected by Map4k4 loss are known Ras target genes (35), and Ras/Erk activation is known to enhance proliferation rather than to induce growth arrest in endothelial cells (36, 37), suggesting that Map4k4 mediates its effects on proliferation by modulating G_2/M transition downstream of Ras. MLECs lacking Map4k4 also displayed a more "lymphatic" EC signature than Flox/Flox MLECs (Fig. 5), suggesting that Map4k4 is important for EC quiescence and lymphatic cell fate decisions.

In conclusion, the data presented here demonstrate that endothelial Map4k4 is a critical regulator of lymphatic vascular development. Map4k4 inhibitors are currently being developed for a number of clinical uses (16, 38, 39). Importantly, the studies reported here call the clinical safety of Map4k4 inhibitors into question due to potential lymphatic vascular sequelae, chyle leakage phenotypes, and a potential to promote lymphangiogenesis and tumor metastasis.

ACKNOWLEDGMENTS

We thank Joseph Virbasius, Silvia Corvera, John Keaney, and Nathan Lawson for helpful discussions, Ozlem Senol-Cosar for technical support, and Joseph Virbasius and Marina DiStefano for critical reading of the manuscript. We also thank the UMASS Morphology core for assistance.

This work was supported by NIH grant DK030898 to M.P.C.

We declare no financial conflicts of interest.

R.J.R.F. and M.P.C. designed the research; R.J.R.F., C.-A.G., J.C.Y., and L.V.D. performed the research; S.G. analyzed gene expression data; Y.J.K.E. provided bioinformatics and IT assistance; and R.J.R.F. and M.P.C. wrote the manuscript.

FUNDING INFORMATION

This work, including the efforts of Rachel J. Roth Flach, Chang-An Guo, Laura V. Danai, Joseph Yawe, Sharvari Gujja, Yvonne JK Edwards, and Michael P. Czech, was funded by HHS | NIH | National Institute of Diabetes and Digestive and Kidney Diseases (NIDDK) (DK030898).

REFERENCES

1. **Choi I, Lee S, Hong YK.** 2012. The new era of the lymphatic system: no longer secondary to the blood vascular system. Cold Spring Harb Perspect Med **2:**a006445. http://dx.doi.org/10.1101/cshperspect.a006445.
2. **Randolph GJ, Miller NE.** 2014. Lymphatic transport of high-density lipoproteins and chylomicrons. J Clin Invest **124:**929–935. http://dx.doi.org/10.1172/JCI71610.
3. **Card CM, Yu SS, Swartz MA.** 2014. Emerging roles of lymphatic endothelium in regulating adaptive immunity. J Clin Invest **124:**943–952. http://dx.doi.org/10.1172/JCI73316.
4. **Alitalo K.** 2011. The lymphatic vasculature in disease. Nat Med **17:**1371–1380. http://dx.doi.org/10.1038/nm.2545.
5. **Wang Y, Oliver G.** 2010. Current views on the function of the lymphatic vasculature in health and disease. Genes Dev **24:**2115–2126. http://dx.doi.org/10.1101/gad.1955910.
6. **Wigle JT, Oliver G.** 1999. Prox1 function is required for the development of the murine lymphatic system. Cell **98:**769–778. http://dx.doi.org/10.1016/S0092-8674(00)81511-1.
7. **Wigle JT, Harvey N, Detmar M, Lagutina I, Grosveld G, Gunn MD, Jackson DG, Oliver G.** 2002. An essential role for Prox1 in the induction

of the lymphatic endothelial cell phenotype. EMBO J **21:**1505–1513. http://dx.doi.org/10.1093/emboj/21.7.1505.

8. **Roth Flach RJ, Skoura A, Matevossian A, Danai LV, Zheng W, Cortes C, Bhattacharya SK, Aouadi M, Hagan N, Yawe JC, Vangala P, Menendez LG, Cooper MP, Fitzgibbons TP, Buckbinder L, Czech MP.** 2015. Endothelial protein kinase MAP4K4 promotes vascular inflammation and atherosclerosis. Nat Commun **6:**8995. http://dx.doi.org/10.1038/ncomms9995.
9. **Alva JA, Zovein AC, Monvoisin A, Murphy T, Salazar A, Harvey NL, Carmeliet P, Iruela-Arispe ML.** 2006. VE-cadherin-Cre-recombinase transgenic mouse: a tool for lineage analysis and gene deletion in endothelial cells. Dev Dyn **235:**759–767. http://dx.doi.org/10.1002/dvdy.20643.
10. **Lapinski PE, Kwon S, Lubeck BA, Wilkinson JE, Srinivasan RS, Sevick-Muraca E, King PD.** 2012. RASA1 maintains the lymphatic vasculature in a quiescent functional state in mice. J Clin Invest **122:**733–747. http://dx.doi.org/10.1172/JCI46116.
11. **Baumgartner M, Sillman AL, Blackwood EM, Srivastava J, Madson N, Schilling JW, Wright JH, Barber DL.** 2006. The Nck-interacting kinase phosphorylates ERM proteins for formation of lamellipodium by growth factors. Proc Natl Acad Sci U S A **103:**13391–13396. http://dx.doi.org/10.1073/pnas.0605950103.
12. **Fitzgibbons TP, Kogan S, Aouadi M, Hendricks GM, Straubhaar J, Czech MP.** 2011. Similarity of mouse perivascular and brown adipose tissues and their resistance to diet-induced inflammation. Am J Physiol Heart Circ Physiol **301:**H1425–H1437. http://dx.doi.org/10.1152/ajpheart.00376.2011.
13. **Mortimer PS, Rockson SG.** 2014. New developments in clinical aspects of lymphatic disease. J Clin Invest **124:**915–921. http://dx.doi.org/10.1172/JCI71608.
14. **Petrova TV, Karpanen T, Norrmen C, Mellor R, Tamakoshi T, Finegold D, Ferrell R, Kerjaschki D, Mortimer P, Yla-Herttuala S, Miura N, Alitalo K.** 2004. Defective valves and abnormal mural cell recruitment underlie lymphatic vascular failure in lymphedema distichiasis. Nat Med **10:**974–981. http://dx.doi.org/10.1038/nm1094.
15. **Bazigou E, Lyons OT, Smith A, Venn GE, Cope C, Brown NA, Makinen T.** 2011. Genes regulating lymphangiogenesis control venous valve formation and maintenance in mice. J Clin Invest **121:**2984–2992. http://dx.doi.org/10.1172/JCI58050.
16. **Vitorino P, Yeung S, Crow A, Bakke J, Smyczek T, West K, McNamara E, Eastham-Anderson J, Gould S, Harris SF, Ndubaku C, Ye W.** 2015. MAP4K4 regulates integrin-FERM binding to control endothelial cell motility. Nature **519:**425–430. http://dx.doi.org/10.1038/nature14323.
17. **Su YC, Han J, Xu S, Cobb M, Skolnik EY.** 1997. NIK is a new Ste20-related kinase that binds NCK and MEKK1 and activates the SAPK/JNK cascade via a conserved regulatory domain. EMBO J **16:**1279–1290. http://dx.doi.org/10.1093/emboj/16.6.1279.
18. **Ger M, Zitkus Z, Valius M.** 2011. Adaptor protein Nck1 interacts with p120 Ras GTPase-activating protein and regulates its activity. Cell Signal **23:**1651–1658. http://dx.doi.org/10.1016/j.cellsig.2011.05.019.
19. **Becker E, Huynh-Do U, Holland S, Pawson T, Daniel TO, Skolnik EY.** 2000. Nck-interacting Ste20 kinase couples Eph receptors to c-Jun N-terminal kinase and integrin activation. Mol Cell Biol **20:**1537–1545. http://dx.doi.org/10.1128/MCB.20.5.1537-1545.2000.
20. **Burrows PE, Gonzalez-Garay ML, Rasmussen JC, Aldrich MB, Guilliod R, Maus EA, Fife CE, Kwon S, Lapinski PE, King PD, Sevick-Muraca EM.** 2013. Lymphatic abnormalities are associated with RASA1 gene mutations in mouse and man. Proc Natl Acad Sci U S A **110:**8621–8626. http://dx.doi.org/10.1073/pnas.1222722110.
21. **King PD, Lubeck BA, Lapinski PE.** 2013. Nonredundant functions for Ras GTPase-activating proteins in tissue homeostasis. Sci Signal **6:**re1. http://dx.doi.org/10.1126/scisignal.2003669.
22. **Deng Y, Atri D, Eichmann A, Simons M.** 2013. Endothelial ERK signaling controls lymphatic fate specification. J Clin Invest **123:**1202–1215. http://dx.doi.org/10.1172/JCI63034.
23. **Simons M, Alitalo K, Annex BH, Augustin HG, Beam C, Berk BC, Byzova T, Carmeliet P, Chilian W, Cooke JP, Davis GE, Eichmann A, Iruela-Arispe ML, Keshet E, Sinusas AJ, Ruhrberg C, Woo YJ, Dimmeler S, American Heart Association Council on Basic Cardiovascular Sciences, Council on Cardiovascular Surgery and Anesthesia.** 2015. State-of-the-art methods for evaluation of angiogenesis and tissue vascularization: a scientific statement from the American Heart Association. Circ Res **116:**e99–e132. http://dx.doi.org/10.1161/RES.0000000000000054.
24. **Harvey NL, Srinivasan RS, Dillard ME, Johnson NC, Witte MH, Boyd K, Sleeman MW, Oliver G.** 2005. Lymphatic vascular defects promoted by Prox1 haploinsufficiency cause adult-onset obesity. Nat Genet **37:**1072–1081. http://dx.doi.org/10.1038/ng1642.
25. **Lim HY, Rutkowski JM, Helft J, Reddy ST, Swartz MA, Randolph GJ, Angeli V.** 2009. Hypercholesterolemic mice exhibit lymphatic vessel dysfunction and degeneration. Am J Pathol **175:**1328–1337. http://dx.doi.org/10.2353/ajpath.2009.080963.
26. **Lim HY, Thiam CH, Yeo KP, Bisoendial R, Hii CS, McGrath KC, Tan KW, Heather A, Alexander JS, Angeli V.** 2013. Lymphatic vessels are essential for the removal of cholesterol from peripheral tissues by SR-BI-mediated transport of HDL. Cell Metab **17:**671–684. http://dx.doi.org/10.1016/j.cmet.2013.04.002.
27. **Martel C, Li W, Fulp B, Platt AM, Gautier EL, Westerterp M, Bittman R, Tall AR, Chen SH, Thomas MJ, Kreisel D, Swartz MA, Sorci-Thomas MG, Randolph GJ.** 2013. Lymphatic vasculature mediates macrophage reverse cholesterol transport in mice. J Clin Invest **123:**1571–1579. http://dx.doi.org/10.1172/JCI63685.
28. **Karkkainen MJ, Haiko P, Sainio K, Partanen J, Taipale J, Petrova TV, Jeltsch M, Jackson DG, Talikka M, Rauvala H, Betsholtz C, Alitalo K.** 2004. Vascular endothelial growth factor C is required for sprouting of the first lymphatic vessels from embryonic veins. Nat Immunol **5:**74–80. http://dx.doi.org/10.1038/ni1013.
29. **Karkkainen MJ, Saaristo A, Jussila L, Karila KA, Lawrence EC, Pajusola K, Bueler H, Eichmann A, Kauppinen R, Kettunen MI, Yla-Herttuala S, Finegold DN, Ferrell RE, Alitalo K.** 2001. A model for gene therapy of human hereditary lymphedema. Proc Natl Acad Sci U S A **98:**12677–12682. http://dx.doi.org/10.1073/pnas.221449198.
30. **Makinen T, Adams RH, Bailey J, Lu Q, Ziemiecki A, Alitalo K, Klein R, Wilkinson GA.** 2005. PDZ interaction site in ephrinB2 is required for the remodeling of lymphatic vasculature. Genes Dev **19:**397–410. http://dx.doi.org/10.1101/gad.330105.
31. **Zhang G, Brady J, Liang WC, Wu Y, Henkemeyer M, Yan M.** 2015. EphB4 forward signalling regulates lymphatic valve development. Nat Commun **6:**6625. http://dx.doi.org/10.1038/ncomms7625.
32. **Kawasaki J, Aegerter S, Fevurly RD, Mammoto A, Mammoto T, Sahin M, Mably JD, Fishman SJ, Chan J.** 2014. RASA1 functions in EPHB4 signaling pathway to suppress endothelial mTORC1 activity. J Clin Invest **124:**2774–2784. http://dx.doi.org/10.1172/JCI67084.
33. **Ichise T, Yoshida N, Ichise H.** 2010. H-, N- and Kras cooperatively regulate lymphatic vessel growth by modulating VEGFR3 expression in lymphatic endothelial cells in mice. Development **137:**1003–1013. http://dx.doi.org/10.1242/dev.043489.
34. **Gupta S, Ramjaun AR, Haiko P, Wang Y, Warne PH, Nicke B, Nye E, Stamp G, Alitalo K, Downward J.** 2007. Binding of ras to phosphoinositide 3-kinase p110alpha is required for ras-driven tumorigenesis in mice. Cell **129:**957–968. http://dx.doi.org/10.1016/j.cell.2007.03.051.
35. **Zuber J, Tchernitsa OI, Hinzmann B, Schmitz AC, Grips M, Hellriegel M, Sers C, Rosenthal A, Schafer R.** 2000. A genome-wide survey of RAS transformation targets. Nat Genet **24:**144–152. http://dx.doi.org/10.1038/72799.
36. **Bajaj A, Zheng Q, Adam A, Vincent P, Pumiglia K.** 2010. Activation of endothelial ras signaling bypasses senescence and causes abnormal vascular morphogenesis. Cancer Res **70:**3803–3812. http://dx.doi.org/10.1158/0008-5472.CAN-09-2648.
37. **Srinivasan R, Zabuawala T, Huang H, Zhang J, Gulati P, Fernandez S, Karlo JC, Landreth GE, Leone G, Ostrowski MC.** 2009. Erk1 and Erk2 regulate endothelial cell proliferation and migration during mouse embryonic angiogenesis. PLoS One **4:**e8283. http://dx.doi.org/10.1371/journal.pone.0008283.
38. **Ndubaku CO, Crawford TD, Chen H, Boggs JW, Drobnick J, Harris SF, Jesudason R, McNamara E, Nonomiya J, Sambrone A, Schmidt S, Smyczek T, Vitorino P, Wang L, Wu P, Yeung S, Chen J, Chen K, Ding CZ, Wang T, Xu Z, Gould SE, Murray LJ, Ye W.** 2015. Structure-based design of GNE-495, a potent and selective MAP4K4 inhibitor with efficacy in retinal angiogenesis. ACS Med Chem Lett **6:**913–918. http://dx.doi.org/10.1021/acsmedchemlett.5b00174.
39. **Schroder P, Forster T, Kleine S, Becker C, Richters A, Ziegler S, Rauh D, Kumar K, Waldmann H.** 2015. Neuritogenic militarinone-inspired 4-hydroxypyridones target the stress pathway kinase MAP4K4. Angew Chem Int Ed Engl **54:**12398–12403. http://dx.doi.org/10.1002/anie.201501515.